**EINDHOVEN UNIVERSITY OF TECHNOLOGY**
Department of Mathematics and Computer Science

CASA-Report 12-01
January 2012

# Macroscopic corrosion front computations of sulfate attack in sewer pipes based on a micro-macro reaction-diffusion model

by

V. Chalupecký, T. Fatima, J. Kruschwitz, A. Muntean


Centre for Analysis, Scientific computing and Applications
Department of Mathematics and Computer Science
Eindhoven University of Technology
P.O. Box 513
5600 MB Eindhoven, The Netherlands
ISSN: 0926-4507

# MACROSCOPIC CORROSION FRONT COMPUTATIONS OF SULFATE ATTACK IN SEWER PIPES BASED ON A MICRO-MACRO REACTION-DIFFUSION MODEL

VLADIMÍR CHALUPECKÝ, TASNIM FATIMA, JENS KRUSCHWITZ, AND ADRIAN MUNTEAN

Abstract. We consider a two-scale reaction diffusion system able to capture the corrosion of concrete with sulfates. Our aim here is to define and compute two macroscopic corrosion indicators: typical pH drop and gypsum profiles. Mathematically, the system is coupled, endowed with micro-macro transmission conditions, and posed on two different spatially-separated scales: one microscopic (pore scale) and one macroscopic (sewer pipe scale). We use a logarithmic expression to compute values of pH from the volume averaged concentration of sulfuric acid which is obtained by resolving numerically the two-scale system (microscopic equations with direct feedback with the macroscopic diffusion of one of the reactants). Furthermore, we also evaluate the content of the main sulfatation reaction (corrosion) product—the gypsum—and point out numerically a persistent kink in gypsum's concentration profile. Finally, we illustrate numerically the position of the free boundary separating corroded from not-yet-corroded regions.

## 1. Introduction

1.1. **Background on sulfate corrosion.** Often in service-life predictions of concrete structures (e.g., sewer systems), the effects of chemical and biological corrosion processes are fairly neglected. In sewer systems and wastewater treatment facilities, where high concentrations of hydrogen sulfide, moisture, and oxygen are present in the atmosphere, the deterioration of concrete is caused mainly by biogenic acids. The so-called microbially-induced concrete corrosion in sewer systems has been a serious unsolved problem[1] for long time. The presence of microorganisms such as fungi, algae or bacteria can induce formation of aggressive biofilms on concrete surfaces. Particularly, the sulfuric acid that causes corrosion of sewer crowns is generated by such a complex microbial ecosystem especially in hot environments. The precise role of microorganisms in the context of sulfates attack on concrete (here we focus on sewer pipes) is quite complex and is therefore less understood from both experimental and theoretical points of view; see, e.g., the experimental studies [4] (optimum pH and growth kinetics of four relevant bacterial strains), [11] (characteristics of the crown microbial system), [12] (microbiologically influenced corrosion of natural sandstone), [16] (succession of sulfur-oxidizing bacteria in the bacterial community on corroding concrete), [17] (isolation of *Thiobacillus thiooxidans*), [21] (Hamburg sewers),[24] (air-water transfer of hydrogen sulfide). As a consequence of this, an accurate large-time forecast of the penetration of the sulfate corrosion front is very difficult to obtain.

*Key words and phrases.* Reaction-diffusion system, sulfate corrosion, pH, free boundary, micro-macro transmission condition, multiscale numerical methods.

[1]There are a lot of financial implications if you want to change the network of pipes in a city like Fukuoka. Our statement here is that questions like *Why changing the pipes if corrosion is not so strong yet and therefore the mechanics structure of the network can/could still hold for 5 more years?* can be addressed in a rigorous mathematical multiscale framework. Such an approach would allow a good understanding and prediction at least of extreme situations.

We want to stress the fact that concrete, in spite of its strong heterogeneity, is mechanically a well-understood material with known composition. Also, the cement (paste) chemistry is well understood. However, all cement-based materials (including concrete) involve a combination of "heterogeneous multi-phase material", "multiscale chemistry", "multiscale transport" (flow, diffusion, ionic fluxes, etc.), and "multiscale" mechanics. Having in view this complexity, such materials are *sensu stricto* very difficult to describe, to analyze mathematically, and last but not least, to deal with numerically. We expect that only after the multiscale aspects of such materials are handled properly, good predictions of the large-time behavior may be obtained. This is our path to addressing this corrosion scenario that is often referred to as *the sulfatation problem*.

Before closing these background notes, let us add some remarks [20] on a closely-related topic of acid sulphate soils[2], which might attract the attention of the multiscale research in the near future. Acid sulphate soils are an important class of soils worldwide. Particularly in coastal areas, sediments often contain a large amount of iron sulfide (FeS and/or $FeS_2$). When by drainage the sediment is exposed to air, this iron sulfide will oxidize to iron sulphate ($FeSO_4$). As long as the sediment still contains calcium carbonate ($CaCO_3$), the FeS will react with it, resulting in gypsum ($CaSO_4$) and iron oxide ($Fe_2O_3$). Gypsum, being much more soluble than calcium carbonate, will tend to leach to the ground- and surface-waters. If the $Fe_SO_4$ is no longer removed by reactions with $CaCO_3$ or other materials, it will tend to accumulate, resulting in a drop of the pH below 4. The problematic acid sulphate soil then will have become a reality. Acid sulphate soils were first described in 1886 by the Dutch Chemist Jacob Maarten van Bemmelen, in connection with problems arising in the Haarlemmermeer Polder. Much of the work in this direction is/was done in the tropics, including Indonesia, Vietnam, and Australia; see, e.g., [13].

1.2. **Objectives and structure of the paper.** In order to be able to tackle the biophysics of the problem at a later stage, eventually coupled with the mechanics of the concrete and the actual capturing of the macroscopic fracture initiation, we focus here on a much simpler setting modeling the multiscale transport and reaction of the active chemical species involved in the sulfatation process. Therefore, the approach and results reported here are only preliminary.

Our main objective is twofold: using a multiscale reaction-diffusion system for concrete corrosion (that allows for feedback between micro and macro scales),

- calculate pH profiles and detect the eventual presence of "sudden" pH drops;
- extract from gypsum concentration profiles the approximate position of macroscopic corrosion fronts.

In Section 2, we present the reaction mechanisms taking place in sewer pipes. In Section 3, we give a mathematical description of the problem and we set a two-scale PDE-ODE system. We briefly comment on a few mathematical properties of the model. In Section 4, we approximate a macroscopic pH numerically using a multiscale FD scheme and comment briefly on the numerical results.

## 2. A few notes on the involved chemistry

Our model includes two important features:

- continuous transfer of $H_2S$ from water to air phase and vice versa;
- fast production of *gypsum* at solid-water interface.

We incorporate the Henry's law to model the transfer of $H_2S$ from the water to the air phase and vice versa [2, 24]. The production of gypsum at the solid-water interface is modeled by a non-linear reaction rate, given by (15).

[2]Compared to concrete, soils are much easier to handle. Their mechanics is simpler and their chemistry is often rudimentary, if any.

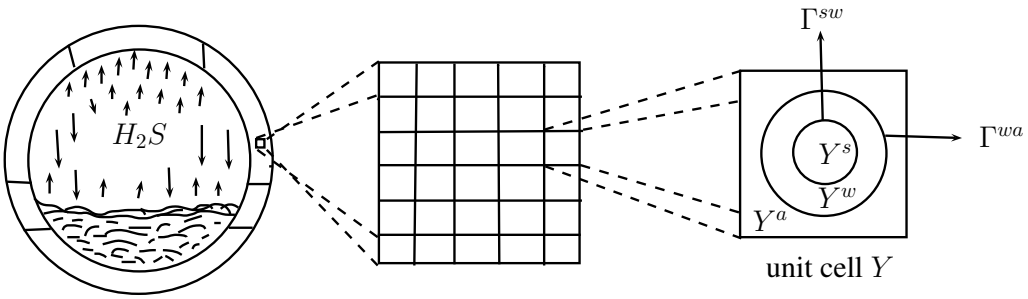


FIGURE 1. Left: Cross-section of a sewer pipe. Middle: Mesoscopic periodic approximation of a REV. Right: Our concept of pore geometry (microstructure).

There are many variants of severe attack to concrete in sewer pipes which influence the performance of concrete structure depending on the intensity of the reactions, the environment, and the turbulence of the wastewater [23]. We focus here on the most aggressive one, namely we consider the following reaction mechanisms causing sulfatation, viz.

$$10\,\mathrm{H}^+ + \mathrm{SO}_4^{2-} + \text{org. matter} \to \mathrm{H_2S(aq)} + 4\,\mathrm{H_2O} + \text{oxidized matter} \tag{1}$$

$$\mathrm{H_2S(aq)} + 2\,\mathrm{O_2} \to 2\mathrm{H}^+ + \mathrm{SO}_4^{2-} \tag{2}$$

$$\mathrm{H_2S(aq)} \rightleftharpoons \mathrm{H_2S(g)} \tag{3}$$

$$2\,\mathrm{H_2O} + \mathrm{H}^+ + \mathrm{SO}_4^{2-} + \mathrm{CaCO_3} \to \mathrm{CaSO_4 \cdot 2\,H_2O} + \mathrm{HCO_{3-}} \tag{4}$$

Reaction (3) is typically a surface reaction taking place as soon as water and air phases meet together. It plays an important role in transferring the $\mathrm{H_2S}$ from the air phase to the liquid phase where the corrosion actually takes place. For modeling details such as a Henry-like "reaction" mechanism, we refer the reader to [9, 5] and references cited therein.

## 3. Multiscale description of the sulfatation problem

We assume that the geometry of our concrete sample (porous medium) consists of a system of pores periodically distributed inside a three-dimensional cube $\Omega := [a, b]^3$ with $a, b \in \mathbb{R}$ and $b > a$. The exterior boundary of $\Omega$ consists of two disjoint, sufficiently smooth parts: the Neumann boundary $\Gamma^N$ and the Dirichlet boundary $\Gamma^D$. We assume that the pores in concrete are made of stationary water film, air and solid parts in different ratios depending on the local porosity. The reference pore, say $Y := [0, 1]^3$, has three pair-wise disjoint domains $Y^s$, $Y^w$ and $Y^a$ with smooth boundaries $\Gamma^{sw}$ and $\Gamma^{wa}$ as shown in Fig. 1 such that

$$Y = \bar{Y}^s \cup \bar{Y}^w \cup \bar{Y}^a.$$

We refer the reader to [9, 6] for more description of the multiscale geometry of the porous material. For a single scale (macroscopic) approach of a sulfatation scenario, we refer the reader to [1], e.g.

We consider a two-scale system of PDEs and one ODE for unknown functions $u_1 : \Omega \times (0, T) \to \mathbb{R}$, $u_k : \Omega \times Y^w \times (0, T) \to \mathbb{R}$, $k \in \{2, 3\}$, and $u_4 : \Omega \times \Gamma^{sw} \times (0, T) \to \mathbb{R}$ where $(0, T)$ is the time interval. The model under consideration is derived by formal homogenization using different

scalings of the diffusion coefficients in [9] (see also [14]) and is given by

$$\partial_t u_1 - d_1\Delta u_1 = -B\left(Hu_1 - \int_{\Gamma^{wa}} u_2 \,\mathrm{d}\gamma_y\right), \qquad \text{in } \Omega\times(0,T), \tag{5a}$$

$$\beta_2\partial_t u_2 - \beta_2 d_2\Delta_y u_2 = -\Phi_2 k_2 u_2 + \Phi_3 k_3 u_3, \qquad \text{in } \Omega\times Y^w\times(0,T), \tag{5b}$$

$$\beta_3\partial_t u_3 - \beta_3 d_3\Delta_y u_3 = \Phi_2 k_2 u_2 - \Phi_3 k_3 u_3, \qquad \text{in } \Omega\times Y^w\times(0,T), \tag{5c}$$

$$\beta_4\partial_t u_4 = \Phi_4 k_4 \eta(u_3,u_4), \qquad \text{in } \Omega\times\Gamma^{sw}\times(0,T), \tag{5d}$$

where $u_1$ denotes the concentration for $H_2S$ gaseous species, $u_2$ for $H_2S$ aqueous species, $u_3$ for $H_2SO_4$, and $u_4$ for *gypsum* at $\Gamma^{sw}$. The water film is taken here to be stationary. A detailed modeling of the role of water is still open, see, e.g., [19, 3, 22]. $\Delta$ without subscript denotes the Laplace operator with respect to macroscopic variable $x$ and $\Delta_y$ with respect to microscopic variable $y$. $\mathrm{d}\gamma_y$ represents the differential over the surface $\Gamma^{wa}$. $\beta_k > 0$, $k \in \{2,3,4\}$, represents the ratio of the maximum concentration of the $k$-th species to the maximum concentration of $H_2SO_4$, $d_i > 0$, $i \in \{1,2,3\}$, are the diffusion coefficients, $B$ is a dimensionless Biot number which gives the mass transfer rate between water and air phases, and $k_j : Y \to R$, $j \in \{2,3,4\}$, are functions modeling the reaction rate "constants". $\Phi_k$ ($k \in \{2,3,4\}$) are Damköhler numbers corresponding to three distinct chemical mechanisms (reactions). They are dimensionless numbers comparing the characteristic time of the fastest transport mechanism (here, the diffusion of $H_2S$ in the gas phase) to the characteristic timescale of the $k$-th chemical reaction.

The system (5) is supplemented with initial and boundary conditions, which read as

$$u_1(x,0) = u_1^0(x), \qquad \text{on } \Omega\times(0,T), \tag{6}$$

$$u_k(x,y,0) = u_k^0(x,y), \qquad \text{on } \Omega\times Y^w\times(0,T),\ k\in\{2,3\}, \tag{7}$$

$$u_4(x,y,0) = u_4^0(x,y), \qquad \text{on } \Omega\times\Gamma^{sw}\times(0,T), \tag{8}$$

$$u_1 = u_1^D, \qquad \text{on } \Gamma^D\times(0,T), \tag{9}$$

$$n_N\cdot(d_1\nabla u_1) = 0, \qquad \text{on } \Gamma^N\times(0,T), \tag{10}$$

$$n_{wa}\cdot(d_2\nabla_y u_2) = B\left(Hu_1 - \int_{\Gamma^{wa}} u_2\,\mathrm{d}\gamma_y\right), \qquad \text{on } \Omega\times\Gamma^{wa}\times(0,T), \tag{11}$$

$$n_{sw}\cdot(d_2\nabla_y u_2) = 0, \qquad \text{on } \Omega\times\Gamma^{sw}\times(0,T), \tag{12}$$

$$n_{wa}\cdot(d_3\nabla_y u_3) = 0, \qquad \text{on } \Omega\times\Gamma^{wa}\times(0,T), \tag{13}$$

$$n_{sw}\cdot(d_3\nabla_y u_3) = -\Phi_3\eta(u_3,u_4), \qquad \text{on } \Omega\times\Gamma^{sw}\times(0,T), \tag{14}$$

where $n_N$ denotes the outward unit normal vector to $\partial\Omega$ along $\Gamma^N$, and $n_{wa}$ and $n_{sw}$ denote the outward unit normal vectors to $Y^w$ along $\Gamma^{wa}$ and $\Gamma^{sw}$, respectively. Note that the "information" at the micro-scale is connected to the macro-scale situation via the right-hand side of (5a) and via the *micro-macro boundary condition* (11). It is also worth noticing that all involved parameters (except for $H$, $d_3$ and $B$) contain microscopic information. The coefficients $d_3$ and $B$ are effective ones (see [9, 8] for a way of calculating them), while $H$ can be read off from existing macroscopic experimental data.

We consider the following form of the reaction rate $\eta$ at the interface $\Gamma^{sw}$

$$\eta(\alpha,\beta) = \begin{cases} \alpha^p(\bar\beta-\beta)^q, & \text{if } \alpha\ge 0, \beta\ge 0,\\ 0, & \text{otherwise,}\end{cases} \tag{15}$$

where $\bar\beta$ is a known maximum concentration of gypsum at $\Gamma^{sw}$ and $p \ge 1, q \ge 1$ are partial orders of reaction. For more modeling possibilities of choosing $\eta$, see [10]. It is worth noting that

production terms like

$$B\left(Hu_1(t,x) - \int_{\Gamma^{wa}} u_2(t,x,y)\,\mathrm{d}\gamma_y\right)$$

are usually referred in the literature as Henry's or Raoult's law, where $H > 0$ is known Henry's constant.

We refer the reader to [6, Theorem 3] for statements regarding the global existence and uniqueness a weak solution to problem (5)–(14) (see also [15] for the analysis on a closely related problem).

## 4. Simulation at a macroscopic pH scale. Capturing free boundaries

In this section the model (5) is applied to the simulation of the acid corrosion due to a microbiotical layer on a cement specimen. We focus on extracting the position of the corrosion front and on the acid reaction, which we use to obtain macro-scale profiles of pH. Both of these results can be compared to experimental data published, e.g., in [11, 16].

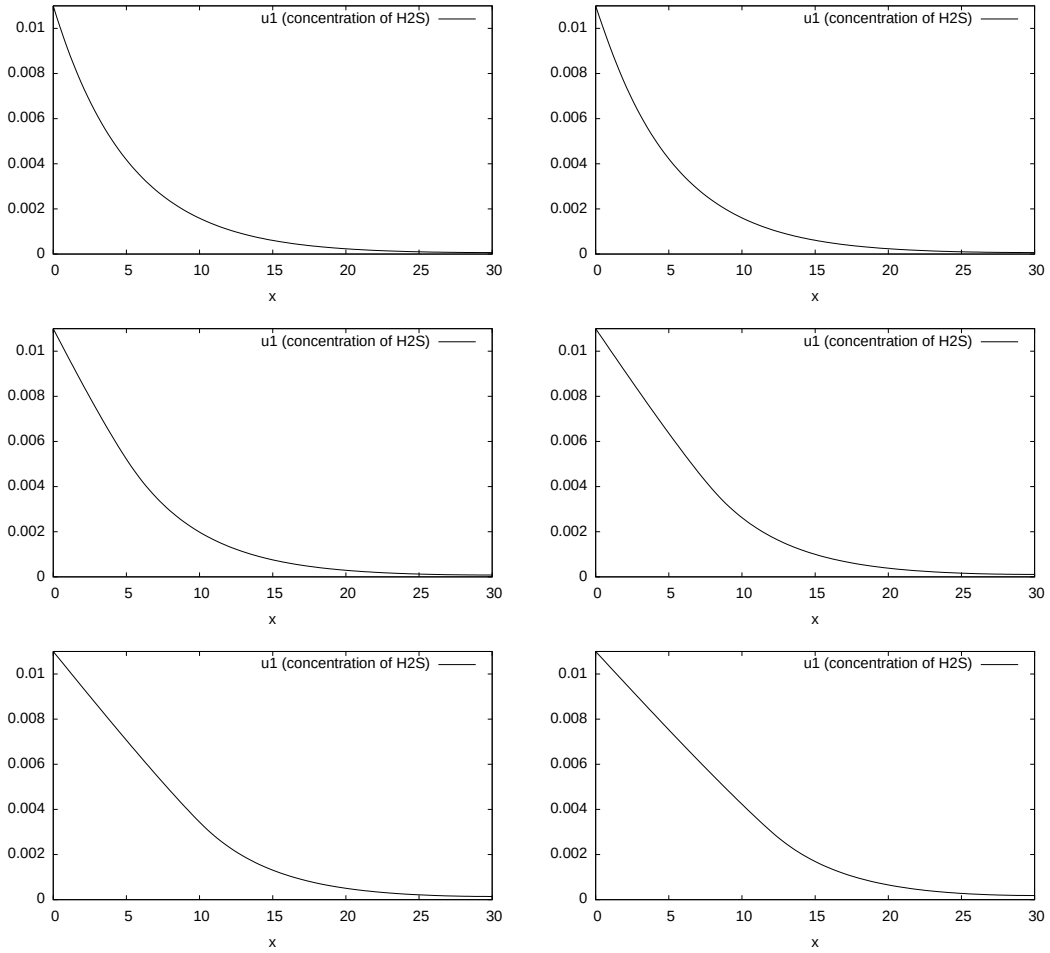


FIGURE 2. Time evolution of $u_1$ (concentration of $H_2S(g)$) shown at $t \in \{2000, 4000, 8000, 12000, 16000, 20000\}$ in left-right and top-bottom order.

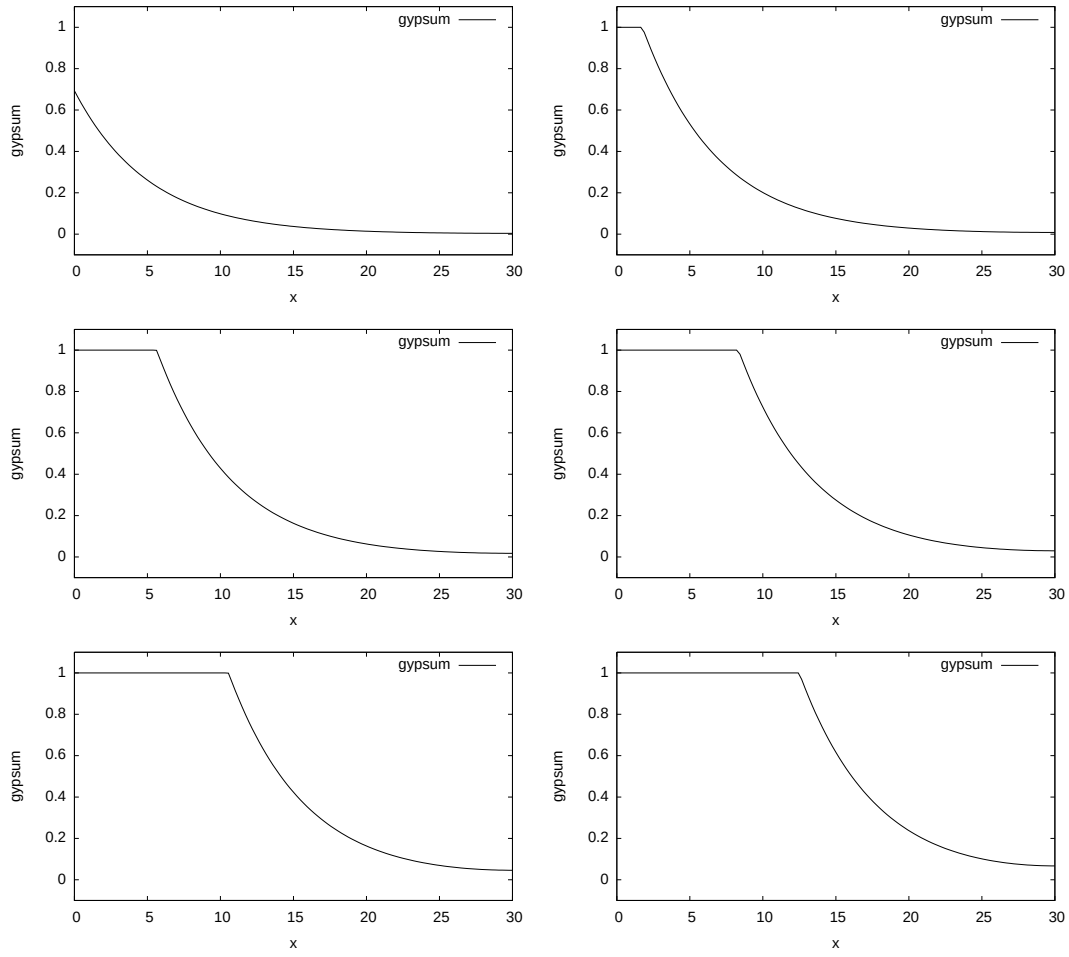


FIGURE 3. Time evolution of $u_4$ (gypsum) shown at $t \in \{2000, 4000, 8000, 12000, 16000, 20000\}$ in left-right and top-bottom order.

For the purpose of the simulation we employ a numerical scheme for a reduced 1D/2D version of the system (5). The reduction consists in taking $\Omega := (0, L)$ and $Y^w = (0, \ell)$ as one-dimensional intervals, which in effect corresponds to analysing the specimen in a perpendicular direction to its surface away from edges and to simplifying the micro cell geometry, respectively. The numerical scheme is based on the method of lines, where in space we use finite difference discretization and in time we employ an implicit higher-order time integrator for the solution of the non-linear ODE system. See [6, 7] for further details of the numerical scheme, its analysis with respect to convergence to the weak solutions and some basic numerical experiments. For details of a computer implementation of the numerical scheme we refer the reader to [14, Chapter 7].

In Table 1 we summarize values of the model parameters used in the simulations described below.

4.1. **Free boundaries.** Figures 2 and 3 show the evolution of $u_1(x, t)$ and $u_4(x, t)$ in time. The Dirichlet boundary condition $u_1(0, t) = u_1^D$ models a constant inflow of $H_2S(g)$ at $x = 0$, i.e., at the surface of the specimen. As the gas diffuses through the porous structure, it enters the

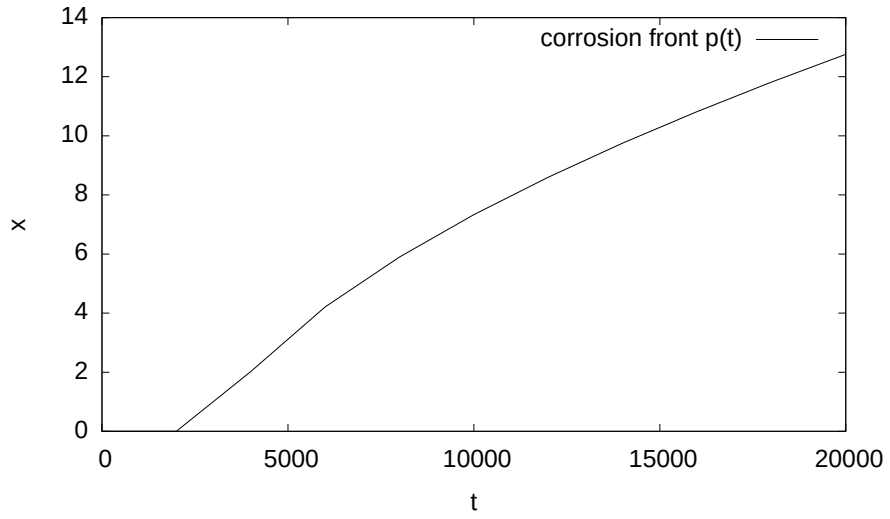


FIGURE 4. Position of the corrosion front.

| $d_1$ | $d_{2,3}$ | $k_2$ | $k_3$ | $k_4$ | $\Phi_{2,3,4}$ | $B$ | $H$ | $\bar{\beta}$ | $p$ | $q$ | $u_1^D$ | $L$ | $\ell$ |
|---|---|---|---|---|---|---|---|---|---|---|---|---|---|
| 0.864 | 0.00864 | 1.48 | 0.0084 | 10 | 1 | 86.4 | 0.3 | 1 | 1 | 1 | 0.011 | 30 | 1 |

TABLE 1. Parameter values used in the numerical simulation.

water film in the pores due to the reaction (3), where it undergoes biogenic oxidation to sulfuric acid. Consequently, its concentration decreases with increasing depth. As the system becomes saturated and as the sulfatation reaction (4) converts available cement into gypsum, the total concentration of $H_2S(g)$ starts to increase (Fig. 2).

Sulfuric acid that arises from the oxidation of $H_2S(aq)$ then reacts at $y = \ell$ with the cement paste and converts it into gypsum ($u_4$) whose concentration profile is shown in Fig. 3. Interestingly, although the behavior of $u_1$ is as expected (i.e., purely diffusive), we notice that a *macroscopic* gypsum layer (region where $u_4$ is produced) is formed around $t = 1500$ and grows in time. The figure clearly indicates that there are two distinct regions separated by a slowly moving intermediate layer: the left region—the place where the gypsum production reached saturation (a threshold), and the right region—the place of the ongoing sulfatation reaction (4) (the gypsum production has not yet reached here the natural threshold).

We use $u_4$ to extract an approximate position of the corrosion front $p(t)$ which we define as (in our scenario, we expect $u_4$ to be decreasing)

$$p(t) := \{x \in (0, L) \mid u_4(x, t) = \bar{\beta} - \varepsilon\},$$

where $\varepsilon$ is a small parameter. Figure 4 shows a graph of $p(t)$ arising from our numerical experiment. We notice that as the corroding front advances further into the concrete specimen, its rate of growth decreases. This is in agreement with experimental data since the hydrogen sulfide gas supplied from the outside environment has to be transported (by diffusion) over ever larger distance. It is important to note that the precise position of the separating layer is *a priori unknown* and to capture it simultaneously with the computation of the concentration profile would require a moving-boundary formulation similar to the one reported in [5].

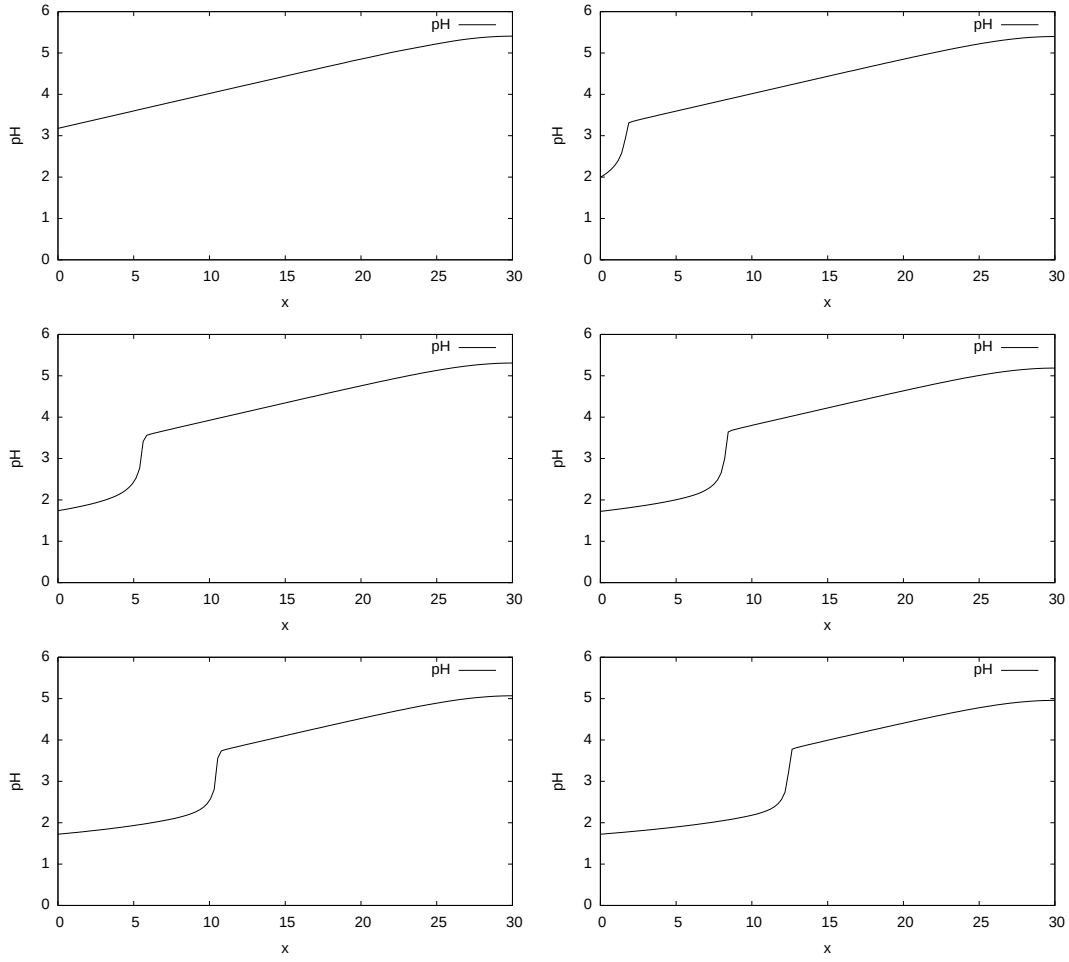


FIGURE 5. Time evolution of macro-scale pH profiles computed from micro-scale information shown at $t \in \{2000, 4000, 8000, 12000, 16000, 20000\}$ in left-right and top-bottom order.

4.2. **Drop in pH.** Emission of hydrogen sulfide from the wastewater to the air space of sewer pipe is an important process because the problems of hydrogen sulfide in sewer pipes are associated with gaseous hydrogen sulfide. Hydrogen sulfide is a weak acid with a dissociation constant of 7.0 (at 20°C) and only the non-dissociated form is emitted in the air space sewer pipe. The pH of the wastewater is therefore of importance when evaluating the potential hydrogen sulfide emission. After the hydrogen sulfide arrives at and diffuses into the concrete, the oxidation of hydrogen sulfide is biological once the pH of the solid matrix has dropped below approximately 8–9 [18]. This represents the tendency of hydronium ions to interact with other components of the solution, which affects among other things the electrical potential read using a pH meter. The concentration of hydrogen ions is expressed as pH scale and pH is defined as a negative decimal logarithm of the concentration of hydronium ions dissolved in a solution.

As the model considered in this paper contains information both from micro (pore) scale and macro-scale, we need a way of computing macro-scale values of pH from the available micro-scale data. Such information is not readily available in the system (5). However, sulfuric acid is a diprotic acid with two stages of dissociation, where the first stage occurs fully and the dissociation in the second stage can be neglected. Therefore, the concentration of hydronium ions is proportional to the concentration of sulfuric acid, which is represented by $u_3$ in our model. We extract the macro-scale concentration of sulfuric acid at each $x$ by taking a volume average of $u_3$ over $Y^w$. Thus, we use the following expression for computing macroscopic pH:

$$\mathrm{pH}_{\mathrm{macro}}(x,t) = -\log_{10}\left(\frac{k_a}{|Y^w|}\int_{Y^w} u_3(x,y,t)\,\mathrm{d}y\right), \tag{16}$$

where $k_a$ is the activity of hydronium ions.

The macro-scale pH profile computed using the formula (16) is shown in Figure 5. We can see that at the beginning of the simulation (first graph) with increasing depth the pH also increases from acid to more basic values as expected. Once all the available cement is consumed and converted into gypsum (this happens for the first time at $x = 0$ between the first and second graph in Figure 5 around $t = 1500$), the pH drops rapidly across the corrosion front. This is due to the fact that behind the corrosion front the sulfuric acid is no longer neutralised by the sulfatation reaction (4).

Note that our pH profiles are not in the experimental range. We expect the size of the drop will become comparable to the one seen in experiments as soon as effects of nonlinear moisture transport and bacteria motility and chemical activity are taken into account in the model equations. The main message that we want to draw is that we are able to detect and compute a macroscopic pH drop, once the needed micro-information is available.

## Acknowledgments

We thank Peter Raats (Wageningen), Hans Kuipers (Eindhoven) and Varvara Kouznetsova (Eindhoven) for useful discussions on this topic during a multiscale symposium that took place in Eindhoven in September 2011.

## References

1. D. Agreba-Driolett, F. Diele, and R. Natalini, *A mathematical model for the $SO_2$ aggression to calcium carbonate stones: Numerical approximation and asymptotic analysis*, SIAM J. Appl. Math. **64** (2004), no. 5, 1636–1667.
2. P. W. Balls and P. S. Liss, *Exchange of $H_2S$ between water and air*, Atmospheric Environment **17** (1983), no. 4, 735–742.
3. R. E. Beddoe and H. W. Dorner, *Modelling acid attack on concrete: Part 1. The essential mechanisms*, Cement and Concrete Research **35** (2005), 2333–2339.
4. A. Bielefeldt, Ma. Guadalupe D. Gutierrez-Padilla, S. Ovtchinnikov, J. Silverstein, and M. Hernandez, *Bacterial kinetics of sulfur oxidizing bacteria and their biodeterioration rates of concrete sewer pipe samples*, Journal of Environmental Engineering **136** (2010), no. 7, 731–738.
5. M. Böhm, F. Jahani, J. Devinny, and G. Rosen, *A moving-boundary system modeling corrosion of sewer pipes*, Appl. Math. Comput. **92** (1998), 247–269.
6. V. Chalupecký, T. Fatima, and A. Muntean, *Multiscale sulfate attack on sewer pipes: Numerical study of a fast micro-macro mass transfer limit*, Journal of Math-for-Industry **2** (2010), no. 2010B–7, 171–181.
7. V. Chalupecký and A. Muntean, *Semi-discrete finite difference multiscale scheme for a concrete corrosion model: approximation estimates and convergence*, Japan J. Indust. Appl. Math. (2012), accepted.
8. C. Eck, *Homogenization of a phase field model for binary mixtures*, Multiscale Model. Simul. **3** (2004), no. 1, 1–27.
9. T. Fatima, N. Arab, E. P. Zemskov, and A. Muntean, *Homogenization of a reaction-diffusion system modeling sulfate corrosion in locally-periodic perforated domains*, J. Engng. Math. **69** (2010), no. 2–3, 261–276.
10. T. Fatima and A. Muntean, *Sulfate attack in sewer pipes: Derivation of a concrete corrosion model via two-scale convergence*, Non-linear Analysis: Real World Applications (2012), submitted/in press.

11. R.L. Islander, J.S. Devinny, F. Mansfeld, A. Postyn, and H. Shih, *Microbial ecology of crown corrosion in sewers.*, J. Environ. Eng. **117** (1991), no. 6, 751–770.
12. R. Mansch and E. Bock, *Untersuchung der Beständigkeit von keramischen Werkstoffen.*, Werkstoffe und Korrosion **45** (1994), 96–104.
13. R. Miller, R. Correll, J. Vanderzalm, and P. Dillon, *Modeling of movement of contaminants from sewer leaks and public open space through the unsaturated zone to the watertable*, CSIRO Report CMIS 05/41, CSIRO, Australia, 2005.
14. A. Muntean and V. Chalupecký, *Homogenization method and multiscale modeling*, MI Lecture Note Series, vol. 34, Kyushu University, GCOE Program, 2011.
15. A. Muntean and M. Neuss-Radu, *A multiscale Galerkin approach for a class of nonlinear coupled reaction–diffusion systems in complex media*, Journal of Mathematical Analysis and Applications **371** (2010), no. 2, 705–718.
16. S. Okabe, M. Odagiri, T. Ito, and H. Satoh, *Succession of sulfur-oxidizing bacteria in the microbial community on corroding concrete in sewer systems*, Appl. Env. Microb. **73** (2007), no. 3, 971–980.
17. C. D. Parker, *The corrosion of concrete. 1. Isolation of a species of bacterium associated with the corrosion of concrete exposed to atmospheres containing hydrogen sulphide.*, The Australian Journal of Experimental Biology and Medical Science **23** (1945), no. 3, 81–90.
18. ———, *Species of sulphur bacteria associated with the corrosion of concrete*, Nature **159** (1947), no. 4039, 439–440.
19. P. A. C. Raats, *Accumulation and transport of water and solutes in saturated and unsaturated zones.*, Hydrochemical balances of freshwater systems. Proc. of the Uppsala Symposium (E. Eriksson, ed.), IAHS Publ. No 150, 1984, pp. 343–357.
20. ———, Personal communication, 2011.
21. W. Sand and E. Bock, *Concrete corrosion in the Hamburg sewer systems.*, Environ. Technol. Lett. **5** (1984), 517–528.
22. R. Tixier, B. Mobasher, and M. Asce, *Modeling of damage in cement-based materials subjected to external sulfate attack. i: Formulation*, J. of Materials in Civil Engineering **15** (2003), 305–313.
23. C. Yongsiri, J. Vollertsen ans M. Rasmussen, and T. Hvitved-Jacobsen, *Air-water transfer of hydrogen sulfide: An approach for application in sewer networks*, Water Envir. Research **76** (2004), no. 81, 81–88.
24. C. Yongsiri, J. Vollertsen, and T. Hvitved-Jacobsen, *Effect of temperature on air-water transfer of hydrogen sulfide*, Journal of Environmental Engineering **130** (2004), no. 1, 104–109.

Institute of Mathematics for Industry, Kyushu University, Japan
*E-mail address*: chalupecky@imi.kyushu-u.ac.jp

Centre for Analysis, Scientific Computing, and Applications, Department of Mathematics and Computer Science, Eindhoven University of Technology, The Netherlands
*E-mail address*: t.fatima@tue.nl

Strassen.NRW, Gelsenkirchen, Germany
*E-mail address*: jens.kruschwitz@strassen.nrw.de

Centre for Analysis, Scientific Computing, and Applications, Department of Mathematics and Computer Science, Institute for Complex Molecular Systems, Eindhoven University of Technology, The Netherlands
*E-mail address*: a.muntean@tue.nl

**PREVIOUS PUBLICATIONS IN THIS SERIES:**

| Number | Author(s) | Title | Month |
|---|---|---|---|
| 11-54 | J. Hulshof<br>R. Nolet<br>G. Prokert | Existence of solutions to the diffusive VSC model | Nov. '11 |
| 11-55 | N. Ray<br>A. Muntean<br>P. Knabner | Rigorous homogenization of a Stokes-Nernst-Planck-Poisson problem for various boundary conditions | Nov. '11 |
| 11-56 | A. Fuster<br>J. van de Sande<br>L.J. Astola<br>C. Poupon<br>J. Velterop<br>B.M. ter Haar Romeny | Fourth-order tensor invariants in high angular resolution diffusion imaging | Nov. '11 |
| 11-57 | J.D. Evans<br>A. Fernández<br>A. Muntean | Single and two-scale sharp-interface models for concrete carbonation – Asymptotics and numerical approximation | Dec. '11 |
| 12-01 | V. Chalupecký<br>T. Fatima<br>J. Kruschwitz<br>A. Muntean | Macroscopic corrosion front computations of sulfate attack in sewer pipes based on a micro-macro reaction-diffusion model | Jan. '12 |

Ontwerp: de Tantes,
Tobias Baanders, CWI